Cement & Concrete Composites 31 (2009) 204–210

Contents lists available at ScienceDirect

Cement & Concrete Composites

journal homepage: www.elsevier.com/locate/cemconcomp

Flexural response of FRC corbels

Giuseppe Campione *

Università di Palermo, Dipartimento di Ingegneria Strutturale e Geotecnica, Viale delle Scienze 90128, Italy

ARTICLE INFO

Article history:
Received 19 May 2008
Received in revised form 4 January 2009
Accepted 7 January 2009
Available online 20 January 2009

Keywords:
Corbels
Reinforced concrete
Steel fibers
Shear strength
Load–deflection curves

ABSTRACT

A strut-and-tie macro-model is proposed to determine the flexural response of fiber reinforced concrete (FRC) corbels, reinforced with longitudinal bars and subjected to vertical load. The effects of the corbel geometry, the percentage of steel fibers, and grades of concrete and steel bars are also included. The model, which is specific for FRC corbels with hooked steel fibers, allows the determination of load levels, and corresponding displacements, associated with the first cracking, yielding of the main steel bars and crushing of the concrete strut. The sequential occurrence of these phenomena is established, depending on the amounts of steel fibers and reinforcing steel.

The simplified flexural response of corbels, in terms of load–deflection curves, is in good agreements with experimental data collected from the literature. In addition, prevision of bearing capacity and failure modes (yielding of main steel or crushing of concrete strut) is obtained with reference to other experimental data collected from the literature. Finally, some recommendations on the design of FRC corbels are given.

1. Introduction

Corbels are structural members whose main function is the transfer of vertical and horizontal forces to principal members (beams, columns, etc.). Many studies presented in the literature [1–7] address the experimental and analytical determination of strength of such elements, and highlighting the role of the parameters governing the structural behavior of corbels including the shape and dimension of corbels, the type and percentage of longitudinal and transverse steel reinforcements and the strength of concrete.

Eurocode 2 [8] and ACI Code [9] provisions consider corbels and give clear indications for the evaluation of their shear strength. A macro strut-and-tie softening model is generally assumed to determine the bearing capacity of corbels. These codes [8,9] also introduce limitations on the geometry of corbels, on the minimum and maximum percentage of reinforcing bars necessary to avoid premature or brittle failure due to the concrete crushing, detailing main and secondary steel reinforcements (Fig. 1).

It has been widely shown that to increase strength and avoid brittle failure due to the crushing of concrete it is necessary to limit the maximum percentage of main steel (see e.g. [8,9]) and to increase the percentage of transverse steel (generally consisting of horizontal stirrups or inclined bars). Recently, it was also observed that good performances are also obtained by integrating or totally substituting the secondary steel reinforcements with the use of fiber reinforced concrete (FRC). The studies referring to the use of FRC for corbels [10–17] stressed that the use of fibers produces significant increases in the bearing capacity and ductility of corbels. Most of the research gives analytical formulae for predicting the bearing capacity, but they do not generally give clear indications for the use of FRC in the design of structures.

In the present paper a strut-and-tie model to predict the load–deflection curves of corbels with main steel and for fiber reinforced concrete is proposed. The main objective of the paper is to give a simple macro-model, which is specific for FRC corbels with hooked steel fibers, able to predict the whole response of FRC corbels and to give indications on the combination of main steel and volume percentage of fiber to adopt in these members to avoid brittle failure. Another objective was also the identification of the range of combination of the mechanical ratio of main steel and fibers to ensure that the structural behavior is mainly governed by the yielding of main steel instead of concrete crushing.

2. Proposed model

The strut-and-tie model presented, initially developed in [15,16] for the calculation of the bearing capacity of corbels reinforced by main and transverse steel bars and in the presence of FRC, is here extended to predict the whole response of corbels in terms of load–deflection curves. In the following sections the model, which is specific for FRC corbels with steel fibers, specifically allows the determination of load levels and the corresponding displacements referring to the first cracking of concrete in tension to the yielding of main steel bars and the crushing of concrete

* Tel.: +39 091 6568467; fax: +39 091 6568407.
E-mail addresses: campione@stru.diseg.unipa.it, campione@diseg.unipa.it

0958-9465/$ - see front matter © 2009 Elsevier Ltd. All rights reserved.
doi:10.1016/j.cemconcomp.2009.01.006

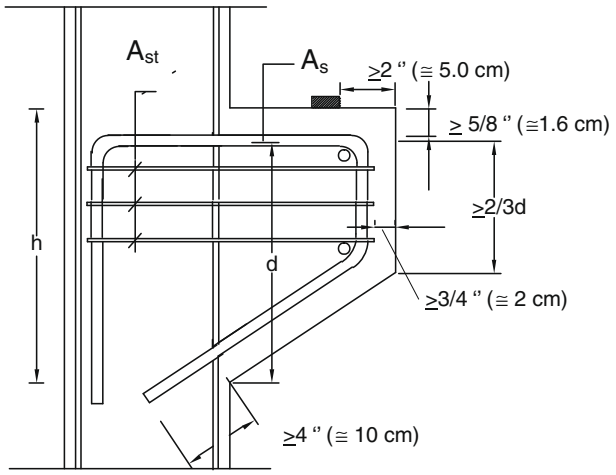

Fig. 1. Steel arrangements in ordinary concrete corbels.

strut, and establishment of the order of occurrence of the above mentioned phenomena depending on the percentage adopted of fibers and main steel.

The case examined is that shown in Fig. 2 of a corbel cast with plain or fiber concrete reinforced with main steel and subjected to a vertical force V applied at distance a from the fixed section. Corbels are reinforced in the tension zone with bars having diameter ϕ and full area A_s covered by a cover δ. Range of a/d ratios considered (with d the depth of corbel and a the shear span) are between 0.4 and 1 which are those suggested in [8]. The geometry of the strut-and-tie model is the one shown in Fig. 2. It consists of a compressed member of concrete, denoted in the following sections as strut member, inclined by an angle α with respect to the horizontal direction, and a member in tension, denoted in the following sections as tie member, constituted by steel bars embedded in the concrete surrounding. The angle α, as shown in Fig. 2, is related to distance between the main bar and the center of the compressed zone (z) measured in the fixed section and to the shear span a by a simple geometrical relation ($\tan\alpha = z/a$).

2.1. Definition of the geometry of the equivalent truss and cross-section analysis of the fixed section

Referring to the geometry and the dimensions of the strut-and-tie member it was assumed that the tie member is formed by the main bars A_s and by the surrounding concrete, the latter having an area:

$$A_c^{\text{eff}} = n \cdot (2 \cdot \delta + \phi)^2 \tag{1}$$

n being the number of main bars adopted.

The strut member consists of a prismatic member having rectangular cross-section of area A_c defined as:

$$A_c = l_{\text{eff}} \cdot b \tag{2}$$

b being the width of the corbels, x_c the neutral axis position in the fixed section and l_{eff} being the effective depth of compressed strut assumed, as already done in [16] with reference to the model of Fig. 2, as:

$$l_{\text{eff}} = x_c \cdot \cos\alpha \tag{3}$$

The cross analysis of the fixed section was made referring to two different conditions of Fig. 3a and b corresponding to the yielding of main bars and to crushing of the concrete region. As shown in Fig. 3a, it was assumed that concrete in compression behaves elastically up to the first yielding of the main steel, as suggested in [16]; while with concrete crushing, a stress block distribution was assumed in the compressed zone as suggested in ACI 544-88 [17]. In both cases the post-cracking tensile strength contribution of material f_{pc} was considered in equilibrium conditions (see Figs. 2 and 3).

The position of the neutral axis x_{cy} at first yielding of the main bars results in the translational equilibrium being written as:

$$\frac{1}{2} \cdot \frac{E_c \cdot f_y}{E_s} \cdot \frac{x_{cy}}{d - x_{cy}} \cdot b \cdot x_c - f_y \cdot A_s - f_{pc} \cdot b \cdot (h - e_y) = 0 \tag{4}$$

The initial tangent elasticity modulus of concrete evaluated according to [18] being E_c.

Analogously with concrete crushing, the equilibrium condition gives the position of neutral axis x_{cu} as:

$$\beta \cdot 0.85 \cdot f_c \cdot b \cdot x_{cu} - f_y \cdot A_s - f_r \cdot b \cdot (d + \delta - e_u) = 0 \tag{5}$$

Being $\beta = 0.80$ for NSC (normal strength concrete) and 0.65 for HSC (high-strength concrete) concretes, as suggested in [18].

In Eqs. (4) and (5) e_y and e_u are the distances between the more compressed fiber of the transverse cross-section and the fiber in which the maximum tensile strength in concrete is reached with first yielding and with concrete crushing (see Fig. 3).

These values can be obtained by considering the plane section hypothesis applied to the fixed section, resulting in:

$$e_y = \frac{\frac{f_t}{E_{ct}} \cdot (d - x_c) + \varepsilon_y \cdot x_{cy}}{\varepsilon_y} \tag{6}$$

E_{ct} being the elasticity modulus of concrete in tension assuming half of E_c as suggested in [19].

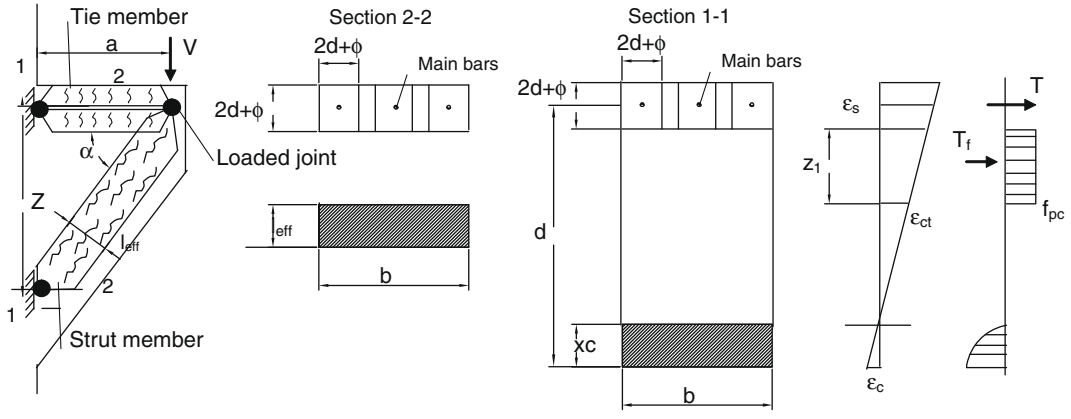

Fig. 2. Truss model and section analysis.

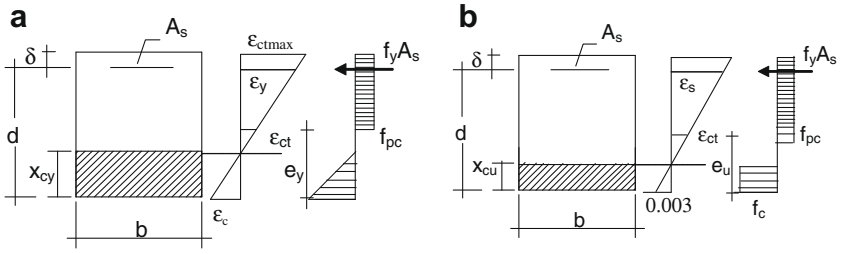

Fig. 3. Cross-section analysis: (a) first yielding and (b) concrete crushing.

The values of x_{cy} and e_y are obtained solving a quadratic equation for position of the neutral axis is obtained in the form:

$$\left[\frac{1}{2}\cdot\frac{E_c\cdot f_y}{E_s}\cdot b + f_{pc}\cdot b\cdot\left(\frac{\varepsilon_{ct}-\varepsilon_y}{\varepsilon_y}\right)\right]\cdot x_{cy}^2 + (f_{pc}\cdot b\cdot\delta + f_y\cdot A_s)\cdot x_{cy} + \left(f_{pc}\cdot b\cdot d^2\cdot\frac{\varepsilon_{ct}}{\varepsilon_y} - f_{pc}\cdot b\cdot h\cdot d - f_y\cdot d\cdot A_s\right) = 0 \quad (7)$$

If the geometrical ratio of main steel $\rho = A_s/(bd)$ is introduced with concrete crushing, the neutral axis position results in:

$$\frac{x_{cu}}{d} = \frac{1}{\alpha}\cdot\frac{\rho\cdot f_y + f_{pc}\cdot\frac{h}{d}}{0.85\cdot f_c + f_{pc}\cdot\frac{f_t/E_{ct}+0.003}{\alpha\cdot 0.003}} \quad (8)$$

$$e_u = x_{cu}\cdot\frac{\frac{f_t}{E_{ct}}+0.003}{0.003} \quad (9)$$

With reference to the maximum and post-cracking tensile strength of FRC with steel fibers, it was shown [16] how it is possible to relate their values to the characteristics of plain concrete and to the geometrical and mechanical characteristics of fibers. In particular the maximum tensile strength and the post-cracking tensile strength can be expressed as:

$$f_{ctf} = f_t\cdot(1-v_f) + 0.033\cdot F\cdot\sqrt{f_c} \cong f_t$$
$$f_{pc} = 0.2\cdot\sqrt{f_c}\cdot F \text{ in MPa} \quad (10)$$

F being the fiber factor expressed as $F = v_f L_f\cdot\lambda/D$, with L_f and D, respectively, the length and diameter of fiber, v_f the volume percentage of fibers and λ a shape factor. This factor is assumed to be 1 for hooked fibers and 0.5 for straight fibers [16]. The tensile strength of plain concrete f_t, as suggested in ACI 318-02 [9], can be assumed as $f_t = 0.7\cdot\sqrt{f_c}$, in MPa.

The distance between the main bar and the center of the compressed zone can be assumed to be:

$$z_y = d - 0.3\cdot x_{cy} \quad \text{at first yielding of main steel}$$
$$z_u = d - 0.4\cdot x_{cu} \quad \text{at concrete crushing} \quad (11)$$

By using Eqs. (4) and (5) it is possible to obtain variation of the neutral axis position with the mechanical ratio of main steel ϖ ($\varpi = \rho\cdot f_y/f_c$) at rupture ($k_u = x_{cu}/d$) and at the first yielding of main steel ($k_y = x_{cy}/d$) for both plain concrete and fiber concrete (see Fig 4). By utilizing Eq. (10) and assuming a volume percentage of fibers equal to 1% and $L_f/D = 60$ for a concrete strength of 60 MPa, a value of post-cracking strength of 1 MPa is obtained for FRC. Minimum and maximum values of mechanical ratios suggested by ACI 318-02 [9] are given in the graph of Fig. 4. Fig. 4 also states that by adding fibers the depth of the neutral axis is increased. For plain concrete the variation of k_y is between 0.12 and 0.20 and the variation k_u is between 0.22 and 0.38. These values for fiber concrete became between 0.15 and 0.25 for first yielding and between and 0.28 and 0.4 for concrete crushing.

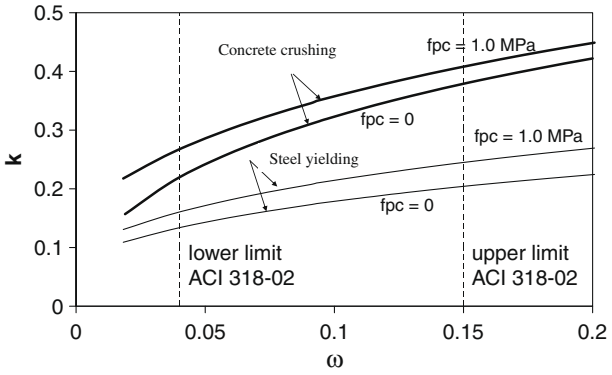

Fig. 4. Variation of neutral axis position with variation of mechanical ratio of main steel.

2.2. Strength and strain capacity of compressed strut and of tie members

To determine the response of tie members, both in terms of strength and strain capacity, elastic–plastic steel bars with strain-hardening response were assumed, while for FRC the model given in [19] was used. This model refers to the tensile response of fiber concrete by means of a stress–strain curve consisting of three linear branches. The first ascending branch reaches the maximum tensile strength with stiffness E_{ct}, the second connects the peak stress with the point having post-cracking strength as its ordinate, and the third horizontal branch characterized by post-cracking strength.

The modulus of elasticity E_s was introduced to define for steel bars the elastic–plastic with strain-hardening behavior, the yielding and the ultimate stresses (f_y,f_u), the corresponding strain values (ε_y,ε_u) and finally the reduced modulus in the strain-hardening phase defined as:

$$E_h = \frac{f_u - f_y}{\varepsilon_u - \varepsilon_y} \quad (12)$$

When considering the member in tension constituted by main bars and concrete surrounding by supposing strain compatibility between steel and concrete, three different stages are considered: the first corresponding to reaching the first cracking strength; the second to reaching the post-cracking tensile; and the last to the yielding of steel bars. The corresponding loads reached in the three different stages are:

First cracking force

$$T_c = A_c^{eff}\cdot f_{ctf} + \varepsilon_{ct}\cdot E_s\cdot A_s \quad (13)$$

Post-cracking force

$$T_{pc} = A_c^{eff}\cdot f_{pc} + \varepsilon_{ct}\cdot E_s\cdot A_s \quad (14)$$

First yielding force

$$T_y = A_c^{eff} \cdot f_{pc} + f_y \cdot A_s \tag{15}$$

For compressed strut the ultimate load can be expressed as:

$$C_u = \xi \cdot f_c' \cdot b \cdot l^{eff} \tag{16}$$

ξ_u being the efficiency factor adopted in strut-and-tie models to take into account the biaxial state of stresses (compression–tension) in the concrete strut and here assumed, as in [20], in the form:

$$\xi = \frac{1}{1 + 0.66 \cdot \left(\frac{a}{z}\right)^2} \tag{17}$$

In the current research Eq. (17) was calculated with reference to the first yielding of the main bar and to the concrete crushing (see Eq. (11)).

By assuming a unit displacement at the tip of the tie for the member in tension (the other tip being supposed as fixed) and deriving the force necessary to produce this displacement, the following values of the stiffness result:

$$R_c = \frac{A_s \cdot E_s}{a}\left(1 + \frac{E_{ct}}{E_s} \cdot \frac{A_c^{eff}}{A_s}\right) \quad \text{at first cracking} \tag{18}$$

$$R_{pc} = \frac{A_f \cdot E_s}{a}\left(1 + \frac{E_r}{E_s} \cdot \frac{A_c^{eff}}{A_s}\right) \quad \text{at post-cracking} \tag{19}$$

$$R_y = \frac{A_s \cdot E_h}{a}\left(1 + \frac{E_{ctr}}{E_h} \cdot \frac{A_c^{eff}}{A_s}\right) \quad \text{at first yielding} \tag{20}$$

E_r being the tangent post-cracking modulus of FRC assumed as f_{pc}/ε_{ctf}.

Two different values of tangent modulus for concrete struts were assumed to define the stiffness of the compressed member, referring to yielding of the main bar and to concrete crushing respectively, in the form:

$$E_c^y = \frac{\xi_y \cdot f_c}{\varepsilon_{c0}} \quad \text{at first yielding} \tag{21}$$

$$E_c^u = \frac{\xi_u \cdot f_c}{\varepsilon_{c0}} \quad \text{at concrete crushing} \tag{22}$$

2.3. Ultimate loads of FRC corbels and corresponding displacements

For the truss structure, already shown in Fig. 2, the equilibrium conditions gives the axial force T in the tie member and the compression force C in the concrete strut expressed, respectively, by:

$$T = \frac{V}{tg\alpha} \quad \text{in the tie member} \tag{23}$$

$$C = \frac{V}{\sin\alpha} \quad \text{in the compressed strut} \tag{24}$$

If the fiber contribution of the tensile zone z_1 (see Fig. 2) is included, the additional contribution to shear strength results in:

$$V_f = \frac{f_{pc} \cdot b \cdot z_1}{2 \cdot \sin 2\alpha} \tag{25}$$

Being z_1 expressed by:

$$z_{1y} = \left(d - \frac{\phi}{2} - x_{cy}\right) \cdot \left(1 - \frac{f_{ct} \cdot E_f}{f_y \cdot E_{ct}}\right) - \delta \quad \text{at first yielding}$$
$$z_{1u} = (d - \frac{\phi}{2} - x_{cu}) \cdot (1 - \frac{f_{ct} \cdot E_f}{f_y \cdot E_{ct}}) - \delta \quad \text{at concrete crushing} \tag{26}$$

Specifically Eq. (26) was derived from considering f_{pc} to be perpendicular to the direction of the strut and acting for a length $z_1/\sin\alpha$ corresponding to the tensile zone z_1 of the fixed cross-section [16].

The shear values corresponding to first cracking, post-cracking, first yielding (including fiber contribution) and crushing of concrete can be obtained by utilizing Eqs. (22) and (24) and substituting the values given by Eqs. (13) and (16) resulting in:

$$V_c = \left(A_c^{eff} + \frac{E_s}{E_{ct}} \cdot A_s\right) \cdot f_{ctf} \cdot \tan\alpha \quad \text{first cracking} \tag{27}$$

$$V_{pc} = \left(A_c^{eff} \cdot f_{pc} + f_{ctf} \cdot \frac{E_s}{E_{ct}} \cdot A_s\right) \cdot \tan\alpha \quad \text{post-cracking} \tag{28}$$

$$V_y = (A_c^{eff} \cdot f_{pc} + f_y \cdot A_s) \cdot \tan\alpha + f_{pc} \cdot b \cdot z_1 \cdot \frac{2}{\sin 2\alpha}$$
first yielding (29)

$$V_u = \frac{1}{2} \cdot \zeta_u \cdot f_c' \cdot b \cdot x_{cu} \cdot \sin 2\alpha + f_{pc} \cdot b \cdot z_1 \cdot \frac{2}{\sin 2\alpha}$$
crushing of concrete (30)

To determine displacement of the loaded joint of the corbel, the compatibility equations for macro strut-and-tie model are first utilized in the form:

$$\delta_s = \varepsilon_s \cdot a \tag{31}$$

$$\delta_c = \varepsilon_c \cdot \sqrt{a^2 + z^2} \tag{32}$$

The elongation of the tie member being δ_s and δ_c corresponding to the compressed strut. To ensure the compatibility of the single truss in the loaded joint the condition has to be verified:

$$\delta_v = \frac{\delta_c}{\sin\alpha} + \frac{\delta_s}{\tan\alpha} \tag{33}$$

Therefore, by substituting Eq. (31) and Eq. (32) in Eq. (33) and utilizing the expression of the displacements δ_c and δ_s obtained by multiplying the stiffness of the members in tension and in compression (see Eqs. (19)–(23)) for the corresponding values of shear forces (see Eqs. (27)–(30)), the following vertical displacements of the loaded joint result:

$$\delta_v^c = \left[\left(\frac{1}{R_c}\right) \cdot \frac{1}{tg^2\alpha} + \frac{\sqrt{a^2 + z^2}}{E_c b \cdot x_c \cos\alpha \cdot \sin^2\alpha}\right] \cdot V_c \quad \text{first cracking} \tag{34}$$

$$\delta_v^y = \left[\left(\frac{1}{R_y}\right) \cdot \frac{1}{tg^2\alpha} + \frac{\sqrt{a^2 + z^2}}{E_c^y b \cdot x_c \cos\alpha \cdot \sin^2\alpha}\right] \cdot V_y \quad \text{first yielding} \tag{35}$$

$$\delta_v^u = \left[\frac{a}{tg\alpha} \cdot \frac{\left(\frac{V_u}{A_f \cdot tg\alpha} - f_y\right)}{E_h} + \frac{\delta_v^y}{\tan\alpha} + \frac{V_u \cdot \sqrt{a^2 + z^2}}{E_c^u \cdot b \cdot x_c \cos\alpha \cdot \sin^2\alpha}\right]$$
crushing of concrete. (36)

It must be noted that, if in the model given in [19] the second branch connecting the peak stress with the point having post-cracking strength as its ordinate is assumed with zero slope for simplicity, Eq. (34) also gives the displacement corresponding to the post-cracking phase because. Eq. (35) in addition gives the ultimate displacements occurring if concrete crushing occurs before the first yielding of main steel. In this case the corresponding displacement is obtained through Eq. (35) replacing V_y with V_c.

Finally, by using Eqs. (27)–(30) with Eqs. (34)–(36), it is possible to plot the trilinear load–deflection curves giving the simplified flexural response of corbels.

3. Comparison with available experimental data

In this section a comparison in terms of load–deflection curves (P–δ_v) is made between the experimental results recently obtained by the author [16] and those obtained with the proposed model. A further comparison is made therefore in terms of bearing capacity

only with other experimental results available in the literature [11–15].

The experimental investigation referred to and developed in detail in [16] considered the flexural response of fiber reinforced corbels. High-strength concrete (HSC) was utilized with compressive strength of 80 MPa and hooked steel fiber with length 30 mm and diameter 0.5 mm at 0.5% and 1% by volume percentage.

Corbels, with $b = 160$ mm and geometry shown in Fig. 5, were reinforced with two longitudinal bars of 10 mm and 16 mm diameter, respectively. Corresponding mechanical ratios were 0.03 for corbels of 2∅ 10 mm and 0.09 for corbels of 2∅ 16 mm. Direct tensile tests carried out on steel bars for 10 and 16 mm diameter, respectively give: yielding stress $f_y = 488$ and 570 MPa; rupture stress $f_u = 601$ and 654 MPa; and ultimate strain ε_u (measured on a gauge length of five equivalent diameters) 18.8% and 16%.

Corbels were tested under flexure according to the loading scheme of Fig. 5 and load–deflection curves (P–δ_v) measured at the loaded point were recorded. The value chosen for a/d was 0.785. During the test the testing machine recorded the whole load P, and it was assumed (in calculation) to be equal to 2 V.

Fig. 6a and b shows the experimental load–deflection curves obtained in [16] for HSC with 2∅ 10 mm and HSC with 2∅ 16 mm both in the absence and presence of fiber at volume percentage of 0.5% and 1.0%. In the same graph analytical results are also given. It should be observed that the proposed model can predict, in an simplified and acceptable manner, the response of corbels in both cases when the tie bars yield before the concrete crushing (when main bars consist of 2∅ 10 mm) and when brittle behavior occurs with failure of the concrete struts before yielding of the steel bars (as occurs when the main bars consist of 2∅ 16 mm). The proposed model can also consider that the addition of fibers increases the initial stiffness and shear strength as well as improving ductility.

By referring to Fig. 6b it can be noted that by using the proposed model which refers to a high percentage of main steel, higher values of first cracking loads are evaluated compared with the experimental values. This phenomenon is due to the proposed model being very stiff (one degree of freedom) and does not take into account the multiple cracking process which occurs in real structures.

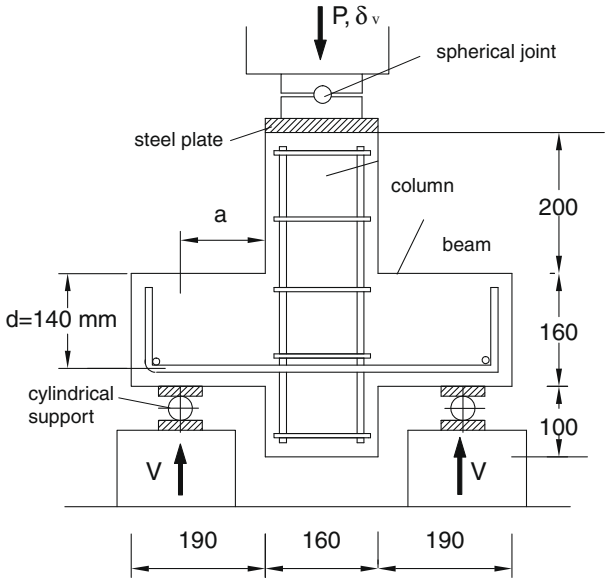

Fig. 5. Load scheme geometry for corbels tested in Campione et al. [16].

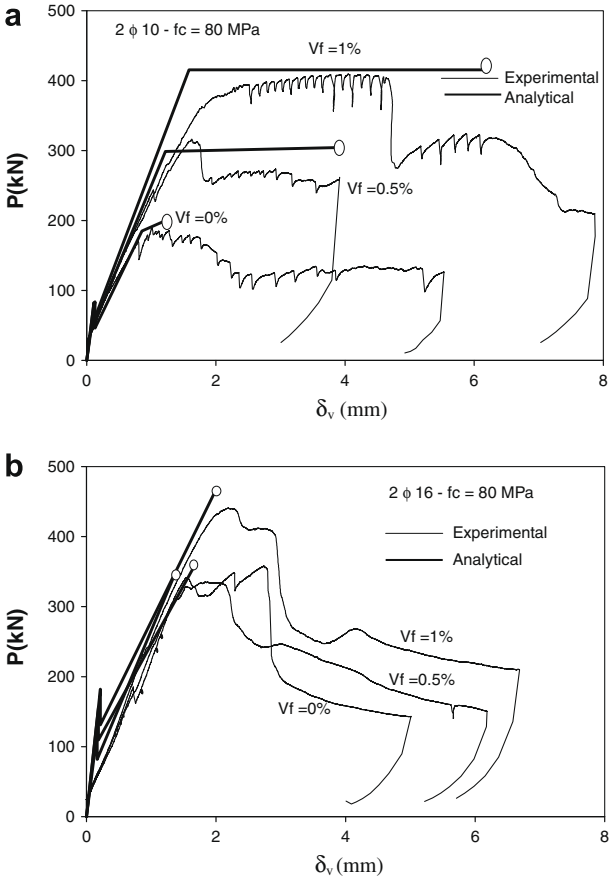

Fig. 6. Load–deflection curves for corbels with $a/d = 0.785$: (a) with 2∅ 10 and (b) with 2∅ 16.

Fig. 7 shows a comparison between the analytical values for shear strength ($v_u = V_u/bd$) predicted with the proposed model and the experimental results collected from the literature [11,12,15]. In the graph of Fig. 7 the predicted value appears in the ordinate and the experimental ones on the abscissa. The analytical prediction with the models proposed in [13,14] is shown in the same graph. The experimental results are 79 data collected for the corbels in fiber concrete. Test data refer to chamfered and non-chamfered corbels. These data refer particularly to; 12 data from [11], 64 data from [12], and 3 data from [15]. The comparison between analytical and experimental results shows good agree-

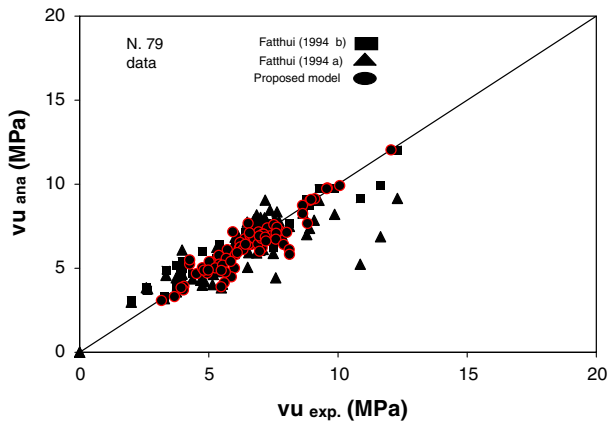

Fig. 7. Comparison between analytical expressions for shear strength of corbels.

ment. Mean values and coefficients of covariation for cases examined were 1.02, and 0.22 for the model of [13], 0.97 and 0.11 for the model [14] and 1.02 and 0.11 according to the proposed model. Results obtained show that all models utilized give good prediction of the experimental results.

4. Code prescriptions and recommendations

Referring to code prescriptions and recommendations, Eurocode 2 [8] prescribes that the area of horizontal main bars A_s must satisfy the relation $A_s \geqslant 0.04 \cdot A_c \cdot \frac{f_{cd}}{f_{yd}}$ in which $A_c = b \cdot h$ is the area of the fixed section of the corbels, and f_{cd} and f_{yd} are the design strength values of concrete and steel, respectively. In addition, in order to reduce the cracking spacing and to produce confinement effects in the compressed strut, horizontal stirrups (or inclined bars) having an area of A_{st} higher than $0.4A_s$ have to be utilized and distributed throughout their depth.

Similar prescriptions are given in ACI 318-02 [9] which prescribe: a minimum amount of mechanical percentage of steel bars expressed by means of ω has to be between 0.04 and 0.15; steel bars distributed within the height of the corbels (secondary reinforcements), situated in a perpendicular direction to the shear force V and placed in the height 2/3 d from the top of the corbel, must consist of least three stirrups, while the gross-area has to be not less than 0.5% $b \cdot d$; stirrups must be bent in a U shape in such way as to wrap the vertical bars situated on the internal side, or if welded to these, anchored appropriately to support to corbels (see Fig. 1).

By utilizing the proposed model (Eqs. (34)–(36)) it can be verified that the mechanical percentages suggested by ACI 318-02 [9] are appropriate for describing the upper limits of the mechanical ratio of main bars to avoid brittle failure and it also allows the derivation of some further comments when utilizing FRC instead of plain concrete.

To do this Fig. 8 shows typical load–deflection curves for high strength plain and fiber concrete corbels with $a/d = 0.8$. Load P represented in the graph is 2 V. The concrete had a compressive strength of 80 MPa and main steel had 460 yielding stress. Typical cases examined refer to two different values of mechanical ratios for main steel of 0.04 and 0.15. For fiber concrete it referred to FRC with hooked steel fibers having an aspect ratio of 60 and post-cracking tensile strength of 1 MPa.

The following considerations, which are in agreement with experimental observations, can be made from the graphs of Fig. 8 when referring to corbels in plain concrete:

– for $\omega = 0.04$ ductile behavior is observed and steel bars yield before concrete crushing, while for $\omega = 0.15$ crushing of concrete is before yielding of the main steel; instances between 0.04 and 0.15 give ductile behavior;

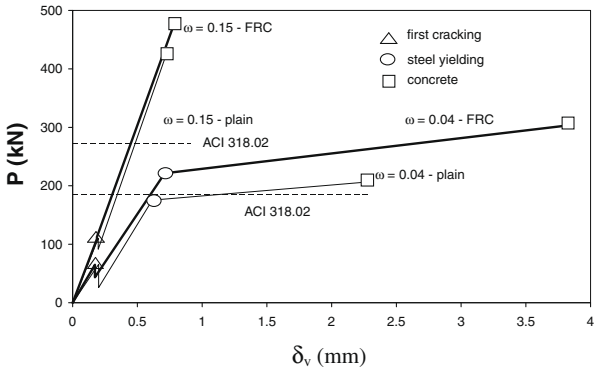

Fig. 8. Simplified load–deflection curves of plain and FRC corbels with main steel.

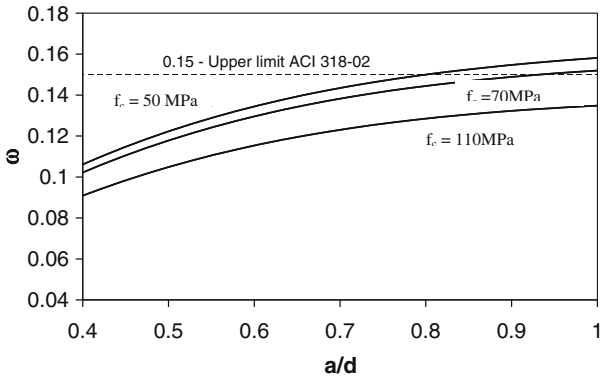

Fig. 9. Variation of maximum mechanical ratio of main steel with a/d ratios.

– strength prediction of shear strength for low and moderate mechanical ratios of main steel obtained with the proposed model are in agreement with the values predicted by ACI 318.02 [9] (see dashed line in the graphs); while for a high percentage of main steel [9] gives a conservative prediction of shear strength. The higher values obtained with the proposed model are in agreement with those obtained by other recent models [7] and with other experimental data.

In the case of FRC corbels:

– the addition of fibers increases the initial stiffness and significantly increases the shear strength;

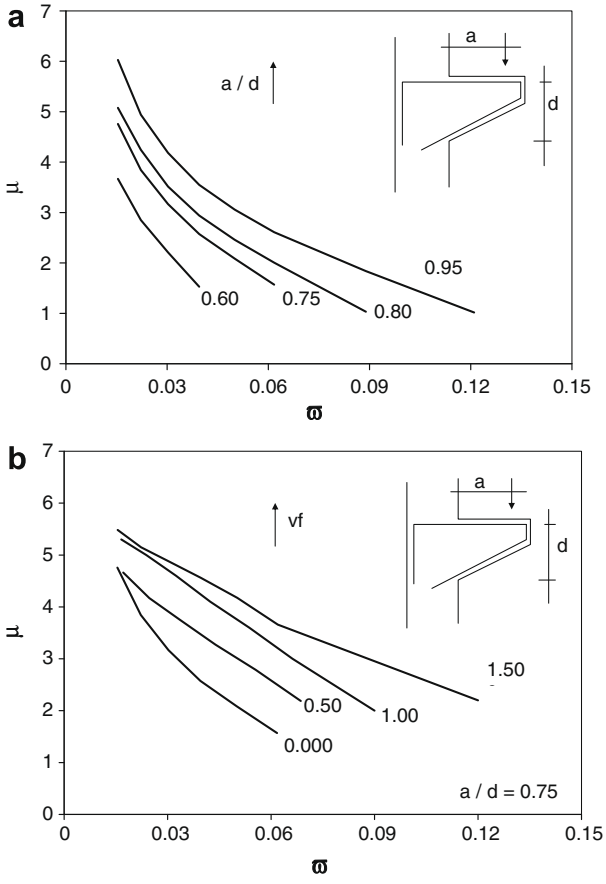

Fig. 10. Variation of ductility factor μ with the mechanical ratio ϖ of main steel for fixed values of: (a) shear to span ration and (b) volume percentages of fibers.

– with a high content of mechanical ratio, the addition of fibers, although increasing significantly the shear strength of corbels, does not allow a change of failure mode from brittle (crushing of concrete) to ductile (yielding of main steel before concrete crushing).

It can be observed that variations in the maximum mechanical ratio ω to ensure the yielding of main steel before the crushing of concrete depends also on a/d values and on concrete strength as shown in Fig. 9. Values of ϖ are obtained for fixed values of a/d, by imposing with the proposed model that the shear force corresponding to first yielding (Eq. (29)) is equal to the shear strength due to concrete crushing (Eq. (30)) for fixed values of compressive strength (values adopted are f_c of 50, 70 and 110 MPa) and deriving the area of main steel and therefore its mechanical ratio. Values of mechanical ratios are in the range of 0.12 and 0.15 for $a/d = 1$, and in the range 0.09 and 0.1 for $a/d = 0.4$. Results obtained show that maximum mechanical ratio has to be further reduced if low a/d ratios are utilized.

Fig. 10a shows variation of the ductility factor μ ($\mu = \delta_u^y/\delta_u^u$) with the mechanical ratios of main steel for different values of a/d ratios and for given compressive strength of 50 MPa. Similarly, Fig. 10b) gives variation of the ductility factor for given values of volume percentages of fibers and $a/d = 0.75$. According to its definition, the ductility factor gives the ratio between the displacements at concrete crushing and the yielding of main bars. If its value is higher than unity, it indicates the ductility resources of corbels. These values of ductility factor were calculated, with the proposed model, as the ratio between the displacement corresponding to concrete crushing (Eq. (36)) and the one corresponding to the first yielding (Eq. (35)).

In the absence of fibers (see Fig. 10a) it must be noted that increasing the mechanical ratio of main bars decrease the ductility factor and in most of the cases examined there is no available ductility. When fibers are added (see Fig. 10b) available ductility increases and the increments are significant, but only when very high percentages of fibers are utilized.

5. Conclusions

A strut-and-tie macro-model is proposed to determine the flexural response in terms of load–deflection curves of fiber reinforced concrete (FRC) corbels reinforced with longitudinal bars and subjected to vertical load. The model takes into account the tensile behavior of main bars embedded in the surrounding fiber concrete and the softening which occurs in the compressed strut, including the effect of percentage of steel fibers, the grade of concrete and the grade and type of steel bars. The simplified flexural response of corbels in terms of load–deflection curves was based on the determination of load levels and the corresponding displacements which refer to the first cracking, to the yielding of main steel and to the crushing of concrete strut.

For corbels cast with ordinary concrete it emerges that with a low content of mechanical ratio of main steel the structural behavior is governed by yielding of the main bars (ductile behavior) while, for high content of mechanical ratio, crushing of concrete occurs before the yielding of main steel and brittle behavior is expected. The addition of fibers increases the initial stiffness and the shear strength significantly, but for a high content of mechanical ratio, although the addition of fibers greatly increases the shear strength of corbels, it does not provide for a change in the mode of failure from brittle (crushing of concrete) to ductile (yielding of main steel before concrete crushing).

Referring to design considerations the proposed model gives: – the variation in the maximum mechanical ratio necessary to ensure the yielding of main steel before the crushing of concrete depends on a/d values and on concrete strength; – and the available ductility with the variation in the shear to span ratios or volume percentages of fibers.

Finally, the model shows good agreement when compared with experimental results recently obtained by the author and with those collected from the literature.

References

[1] Solanki H, Sabnis GM. Reinforced concrete corbels-simplified. ACI Struct J 1987;84(5):428–32.
[2] Yong Y, Balaguru P. Behaviour of reinforced high-strength-concrete corbels. J Struct Eng ASCE 1994;120(4):1182–201.
[3] Foster SJ, Powell RE, Selim HS. Performance of high-strength concrete corbels. ACI Struct J 1996;93(5):555–63.
[4] Choi KK, Reda Taha MM, Park HG, Maji AK. Punching shear strength of interior concrete slab-column connections reinforced with steel fibers. Cem Concr Compos 2007;29(5):409–20.
[5] Hwang S, Lee H. Strength prediction for discontinuity regions by softened strut and tie model. J Struct Eng ASCE 2002;128(12):1519–26.
[6] Foster SJ, Malik AR. Evaluation of efficiency factor models used in strut-and-tie modeling of nonflexural members. J Struct Eng ASCE 2002;128(5):569–77.
[7] Russo G, Venir R, Pauletta M, Somma G. Reinforced concrete corbels shear strength model and design formula. ACI Struct J 2006;103(1):3–7.
[8] Eurocodice 2. Progettazione delle strutture di calcestruzzo (UNI ENV 1992-1-1). Commissione "Ingegneria Strutturale", Milano (Italian Version).
[9] ACI Committee 318. Building code requirements for reinforced concrete (ACI 318-95), and commentary ACI 318RM-02. Detroit, Michigan: ACI; 2002.
[10] Fattuhi NI. SFRC corbel tests. ACI Struct J 1987;84(2):119–651.
[11] Fattuhi NI, Hughes BP. Ductility of reinforced concrete corbels containing either steel fibers or stirrups. ACI Struct J 1989;86(6):644–51.
[12] Fattuhi NI. Strength of SFRC corbels subjected to vertical load. ACI Struct J 1990;116(3):701–18.
[13] Fattuhi NI. Strength of FRC corbels in flexure. J Struct Eng ASCE 1994;120(2):360–77.
[14] Fattuhi NI. Reinforced corbels made with plain and fiber concretes. ACI Struct J 1994;91(5):530–6.
[15] Campione G, La Mendola L, Papia M. Flexural behaviour of concrete corbels containing steel fibers or wrapped with FRP sheets. Mater Struct 2005;38(280):617–25.
[16] Campione G, La Mendola L, Mangiavillano ML. Steel fibers reinforced concrete corbels: experimental behavior and shear strength prediction. ACI Struct J 2007;104(5):570–9.
[17] ACI Committe 544. Design considerations for steel fiber reinforced concrete. ACI Struct J 1988;85(5):563–80.
[18] Dupont D, Vandewalle L. Shear capacity of concrete beams containing longitudinal reinforcement and steel fibers. In: Banthia N, Criswell M, Tatnall P, Folliard K, editors. Innovations in fiber-reinforced concrete for value: ACI SP-216; 2003. p. 78–94.
[19] Mansur MA, Ong KCG. Behavior of reinforced fiber concrete deep beams in shear. ACI Struct J 1991;88(1):98–105.
[20] Collins Mitchell. Rational approach to shear design-the 1984 Canadian code provisions. ACI Struct J 1986;83(6):925–33.